

Three-dimensional architecture of collagen type VI in the human trabecular meshwork

Elena Koudouna,¹ Robert D. Young,¹ Morio Ueno,² Shigeru Kinoshita,² Andrew J. Quantock,¹ Carlo Knupp¹

¹Structural Biophysics Group, School of Optometry and Vision Sciences, Cardiff University, Wales, UK; ²Department of Ophthalmology, Kyoto Prefectural University of Medicine, Hirokoji Kawaramachi, Kyoto, Japan

Purpose: Type VI collagen is a primary component of the extracellular matrix of many connective tissues. It can form distinct aggregates depending on tissue structure, chemical environment, and physiology. In the current study we examine the ultrastructure and mode of aggregation of type VI collagen molecules in the human trabecular meshwork.

Methods: Trabecular meshwork was dissected from donor human eyes, and three-dimensional transmission electron microscopy of type VI collagen aggregates was performed.

Results: Electron-dense collagen structures were detected in the human trabecular meshwork and identified as collagen type VI assemblies based on the three-dimensional spatial arrangement of the type VI collagen molecules, the 105-nm axial periodicity of the assemblies themselves, and their characteristic double bands, which arose from the globular domains of the type VI collagen molecules. Sulfated proteoglycans were also seen to associate with the assemblies either with the globular domain or the inner rod-like segments of the tetramers.

Conclusions: No extended structural regularity in the organization of type VI collagen assemblies within the trabecular meshwork was evident, and the lateral separation of the tetramers forming the assemblies varied, as did the angle formed by the main axes of adjacent tetramers. This is potentially reflective of the specific nature of the trabecular meshwork environment, which facilitates aqueous outflow from the eye, and we speculate that extracellular matrix ions and proteins might prevent a more tight packing of type VI collagen tetramers that form the assemblies.

Type VI collagen is a primary component of the extracellular matrix of many connective tissues [1,2], notably skin [3] and cornea. It was originally identified in pepsin fragments of human aortic intima [4] and designated as “intima collagen.” After further electron microscopy and biochemical studies [3,5], intima collagen was renamed type VI collagen [6] and a detailed structural model for this type of collagen was proposed [7-13].

Type VI collagen is a heterotrimer and was long considered to be composed of three [14] genetically distinct alpha 1 (VI), alpha 2 (VI), and alpha 3 (VI) chains [15]. However, recently three novel collagen VI alpha chains have been discovered in humans: alpha 4 (VI), alpha 5 (VI), and alpha 6 (VI) chains [16,17]. After secretion into the extracellular matrix, the alpha chains assemble as type VI collagen molecules [5] that possess a central collagenous triple-helical segment, about 105 nm long, delimited at both ends by a globular domain (Figure 1A). Pairs of collagen VI molecules coil together in an antiparallel fashion [11] with a 30-nm axial shift to form dimers (Figure 1B) [5]. Two dimers associate

laterally with no axial shift to give rise to a tetramer (Figure 1C) [6], which can be considered as the basic structural unit of collagen VI microfibrils (Figure 1D) [7,18]. Cysteine residues form disulfide bridges between monomers in dimers and between dimers in tetramers [19], and they stabilize the main collagen VI structural unit. Tetramers can be described as possessing an inner rod-like region and two outer rod-like regions separated by and ending with the collagen VI globular domains of the four molecules forming them (Figure 1C).

Unlike the more abundant type I collagen [3], type VI collagen gives rise to cross-banded aggregates that are characterized by a pattern of pairs of transverse bands approximately 30 nm apart with a periodicity of about 105 nm [6,9,18]. In particular, noncovalent bonds between the C- and N-terminal globular domains at each end [6] of the outer rod-like regions of two adjacent tetramers produce end-to-end, cross-banded, pseudofibrillar aggregates (Figure 1D) with a repeated ca. 30–75-nm spacing [5,20]. The same interactions between globular domains of the tetramers also account for the formation of more extended collagen VI aggregates [21] resembling open networks. The basic way in which collagen type VI tetramers can assemble explains the organization of morphologically distinct aggregates [22-24], which also depends on the structure and physiology of the tissue [25-28] in which they are found.

Correspondence to: Andrew Quantock, Structural Biophysics Group, School of Optometry and Vision Sciences, Cardiff University, Maindy Road, Cardiff CF24 4HQ, Wales, UK; Phone: +44 (0)29 20875064; FAX: +44 (0)29 20874859; email: address: QuantockAJ@cf.ac.uk

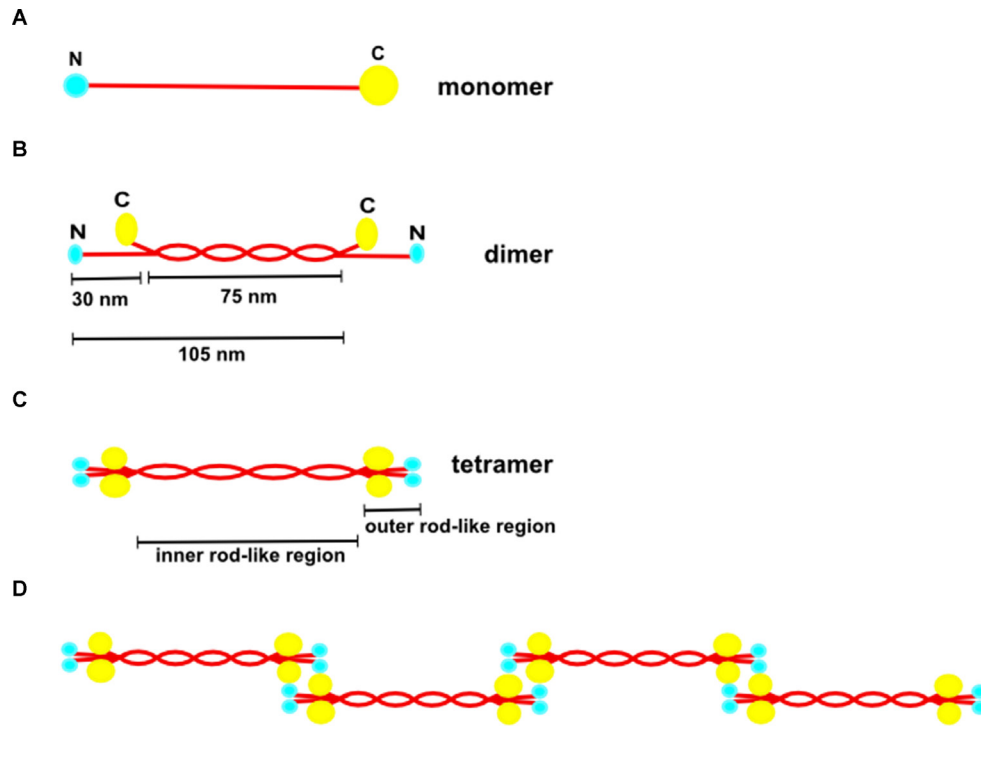


Figure 1. Schematic drawings of the structures of (A) monomer, (B) dimer, (C) tetramer, and (D) microfibrils of type VI collagen. N (NH₂) and C (COOH) are the amino- and carboxy-terminal domains, represented in blue and yellow, respectively. The collagenous triple helices (red in color) associate laterally with a 30-nm axial shift in dimers (B). Pairs of dimers associate laterally to form tetramers (C). Tetramers can be described as possessing an inner rod-like region and two outer rod-like regions separated by and ending with the collagen VI globular domains. Limited resolution of collagen VI fibrils in micrographs causes the globular domains to appear as transverse electron-dense bands (D).

Type VI collagen interacts with extracellular matrix constituents [29,30] in several connective tissues [31-33]. Collagen type VI is associated with several human disorders. For example, individuals having Bethlem myopathy exhibit mutations of the collagen type VI genes (*COL6A1*, *COL6A2*, *COL6A3*) that affect the N- terminal domains [34-36]. Collagen type VI assemblies are also involved with pathogenesis of ocular disorders, including age-related macular degeneration [37] and Sorsby's fundus dystrophy [38]. Here, we examine the three-dimensional organization of collagen type VI aggregates in the human trabecular meshwork (Figure 2), the extracellular matrix of which provides flow resistance to aqueous humor leaving the anterior chamber of the eye [39] and which thus plays a role in the regulation of intraocular pressure.

METHODS

Specimen preparation and transmission electron microscopy: Ocular tissues containing trabecular meshwork were dissected out by one of us (MU, an ocular surgeon) from both eyes of a 69-year-old female donor. Tissue, which was obtained from the Bristol Eye Bank, Bristol, UK, with full informed consent, was immediately fixed in 2.5% glutaraldehyde in 25 mM sodium acetate buffer (pH 5.7) containing 0.1 M MgCl₂ and 0.05% cuproline blue dye (the dye (Polysciences Inc., Warrington, PA) was included to stain sulfated

proteoglycans). Samples were then washed in sodium acetate buffer to remove the glutaraldehyde fixative and cuproline blue dye. Immersion in 0.5% sodium tungstate was performed to add contrast to the stained proteoglycans, and dehydration was accomplished by exposing the tissue to a graded series of ethanol (50%–100%). Following conventional processing with epoxy resin embedding (Agar Scientific, Stansted, UK), ultrathin sections approximately 90 nm thick were cut on an Ultracut E ultramicrotome (Leica Microsystems (UK) Ltd, Milton Keynes, UK) and contrasted for transmission electron microscopy by staining with saturated aqueous uranyl acetate for 12 min followed by four washes in filtered distilled water (1 min per wash). Sections were examined with a JEOL 1010 transmission electron microscope (Jeol UK, Welwyn Garden City, UK) operating at 80 kV. Experiments were conducted in accordance with the ethical principles that have their origin in the Declaration of Helsinki and in line with the requirements of the [UK Human Tissue Act](#).

Electron tomography: For electron tomography, 120-nm-thick sections were cut and collected on naked 200 mesh copper grids. After uranyl acetate staining as indicated above, 10 nm colloidal gold particles (BBI, Cardiff, UK) were deposited on both sides of the grid to serve as fiducial markers. A 92 single-axis tilt series of electron micrographs of collagen type VI assemblies was obtained from +60° to -60° in either 1° and 2° increments. Images were acquired using a Gatan

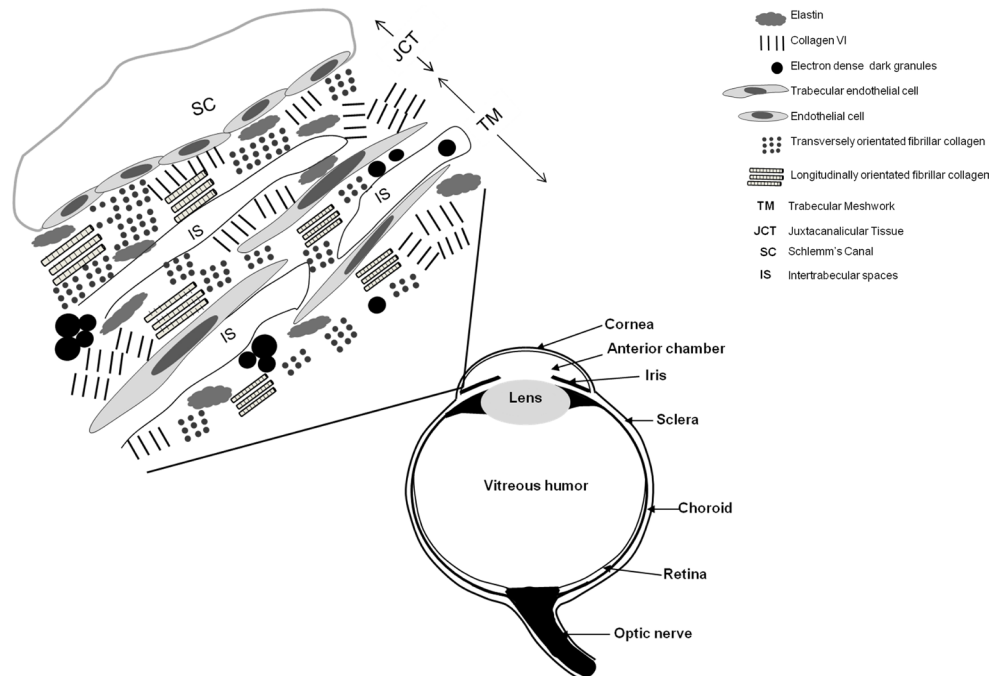


Figure 2. Schematic diagram of the eye showing the major ocular structures and the anatomic positions of the Schlemm's canal (SC), the juxtacanalicular tissue (JCT), and the trabecular meshwork (TM). The corneoscleral region of the TM is separated from SC by a connective tissue layer known as the JCT, which terminates adjacent to a layer of endothelial cells that line the inner wall of SC. The structure of the TM encompasses intertrabecular spaces (IS), trabecular sheets (trabecular beams) filled with extracellular matrix molecules, including elastin, collagens, some

electron-dense dark granules, and thin trabecular endothelial cells. The IS as well as the trabecular sheets (trabecular beams) vary in size and shape.

ORIOUS SC1000 charge coupled device camera (Gatan, Pleasanton, CA) at 20,000X magnification. Micrographs were aligned at a pixel size of 0.4 nm based on the position of the colloidal gold particles on each image. Tomographic reconstructions of longitudinal sections of trabecular meshwork type VI collagen aggregates and stained proteoglycan filaments were generated with the IMOD software package (Boulder, CO) [40]. Segmentation of the tomograms, three-dimensional analysis, and visualization were accomplished via the use of EM3D software (College Station, TX) [41]. Visualization of the reconstructed image stacks and the generation of animated stereo views were achieved with the 3DViewer plug-in of the ImageJ software package (Bethesda, MD) [42,43].

RESULTS

Transverse, banded, collagenous assemblies were found to be widespread throughout the extracellular matrix of the human trabecular meshwork beams and the juxtacanalicular region. These assemblies, displaying an axial periodicity of 109 ± 13 nm (mean \pm standard deviation, $n=47$), formed clusters of different sizes, which often lined the intratrabecular spaces and which were surrounded by interstitial collagen fibrils displaying the typical 67-nm axial periodicity (Figure 2 and Figure 3). These assemblies, from their general appearance and periodicity, closely resembled the assemblies of collagen

VI molecules found in other tissues [21] and matched the 100–120-nm periodicity of presumed type VI collagen long-spacing collagen documented in the human trabecular meshwork [44]. One main difference was that in the trabecular meshwork the transverse bands were single instead of double bands. In typical collagen VI assemblies, the transverse bands arise from the electron dense material of the globular N- and C-terminal domains of the collagen type VI molecules and are split into pairs (Figure 4). These double bands are characteristic and indicative of collagen type VI assemblies and come about as a consequence of the axial alignment of the N- and C-globular domains of the outer rod-like regions of collagen type VI tetramers, which are about 30 nm apart axially (Figure 1C,D).

In the aggregates studied here, as well as in those of collagen VI described previously in other tissues [3,5-13], electron dense filaments were seen running perpendicular, or nearly perpendicular, to the transverse bands and crossing them. In the case of the collagen VI assemblies, these filaments were interpreted as arising from the inner and outer rod-like segments of the type VI collagen tetramers that form the assemblies (Figure 5) [37,38].

The many structural similarities between the assemblies in this study of trabecular meshwork and the collagen VI assemblies examined elsewhere [12,37,38,45] suggested that they were all made of collagen VI, with the tetramers

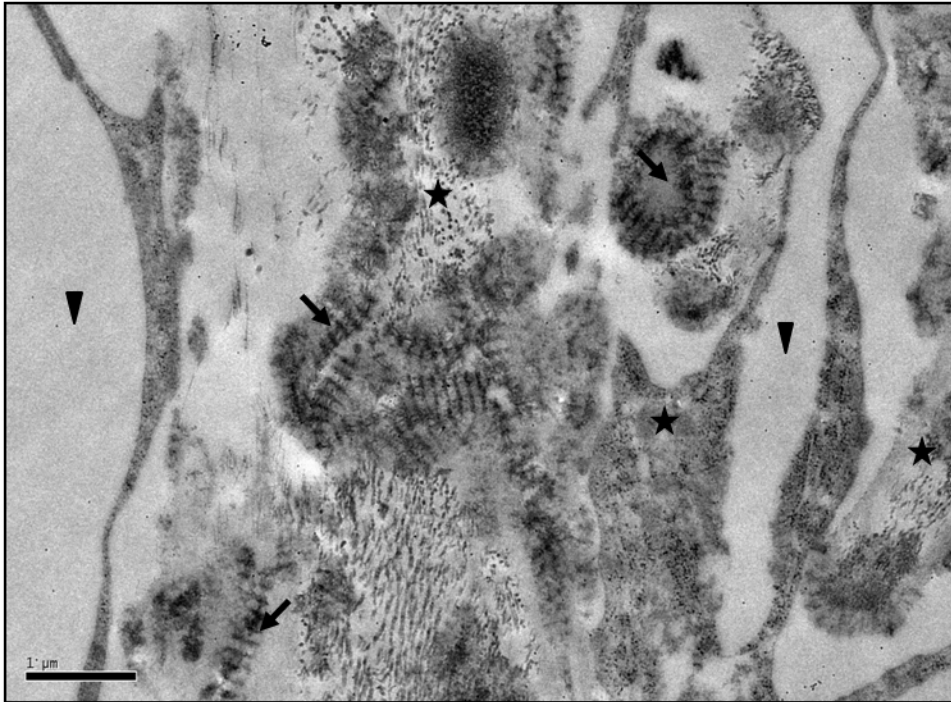


Figure 3. Transmission electron micrograph of the human trabecular meshwork showing a series of parallel layers of connective tissue, known as the trabecular sheets (stars), and intertrabecular spaces forming irregular channels (arrowheads). The trabecular sheets consist of collagen fibrils orientated both transversely and longitudinally and thin trabecular endothelial cells. Type VI aggregates (arrows) are distributed throughout the entire width of the sheet surrounded by collagen fibrils. The black dots dispersed throughout the trabecular meshwork represent 10-nm colloidal gold particles used for tomography. Scale bar = 1 μm .

arranged in essentially the same way. An exhaustive search at the microscope, which included tilting the specimens at different angles, produced clear evidence of single bands splitting into double bands in a small number of assemblies (Figure 4). These double bands were revealed only for a limited tilt angle range, appearing as single transverse bands at a 0° tilt angle, splitting into double bands at higher angles (about 20° in the cases shown in Figure 4), and reverting to single but much narrower bands at higher tilt angles. The axial distance between double bands in these assemblies was not regular, ranging between 112 nm and 85 nm. This would be expected if the tetramers in the assemblies were forming transient links and had not yet settled into a stable configuration. The ratio between the smaller and the larger gaps between the double bands in the most regular assemblies was about 0.2, which is consistent with that of other collagen VI assemblies. The existence of the double bands confirmed the presence of collagen VI in the assemblies.

To achieve a better understanding of the way in which collagen type VI molecules interact with each other in the trabecular meshwork, we generated three-dimensional tomographic reconstructions of the assemblies from single-axis tilt series of electron micrographs. This type of analysis can reveal details of the molecular organization of collagen type VI aggregates that are not accessible from conventional two-dimensional transmission electron microscopy (Figure

5) and can offer new insights into the way collagen type VI molecules are assembled in the matrix of the human trabecular meshwork. In Figure 6 we present one typical three-dimensional reconstruction that we produced of a type VI collagen assembly. Figure 6A shows an 8.57-nm thick slice through the reconstruction, while Figure 6B shows a surface rendering of the same reconstruction. Figure 6C represents a manual segmentation of the same view (see also Appendix 1, Appendix 2, and Appendix 3). In the surface rendering in Figure 6B, the presence of globular domains (highlighted with red arrows) was evident within a transverse band. Globular domains such as these, when not interacting with other material of the extracellular matrix, are likely to be responsible for the double bands seen in typical collagen VI assemblies (and in the assemblies seen in Figure 4). In the trabecular meshwork, the inner rod-like segments of the collagen type VI tetramers assemble with an unsystematic irregular lateral arrangement (Figure 6B; yellow arrowheads), with no evidence of a regular lateral repeat.

Our three-dimensional reconstructions of the trabecular meshwork showed the presence of sulfated proteoglycan filaments, which as well as populating the fibrillar matrix were also seen to co-associate with collagen type VI assemblies (Figure 5, Figure 6, and Appendix 4). The stained filaments were identical in nature to those seen in two-dimensional electron micrographs of trabecular meshwork published

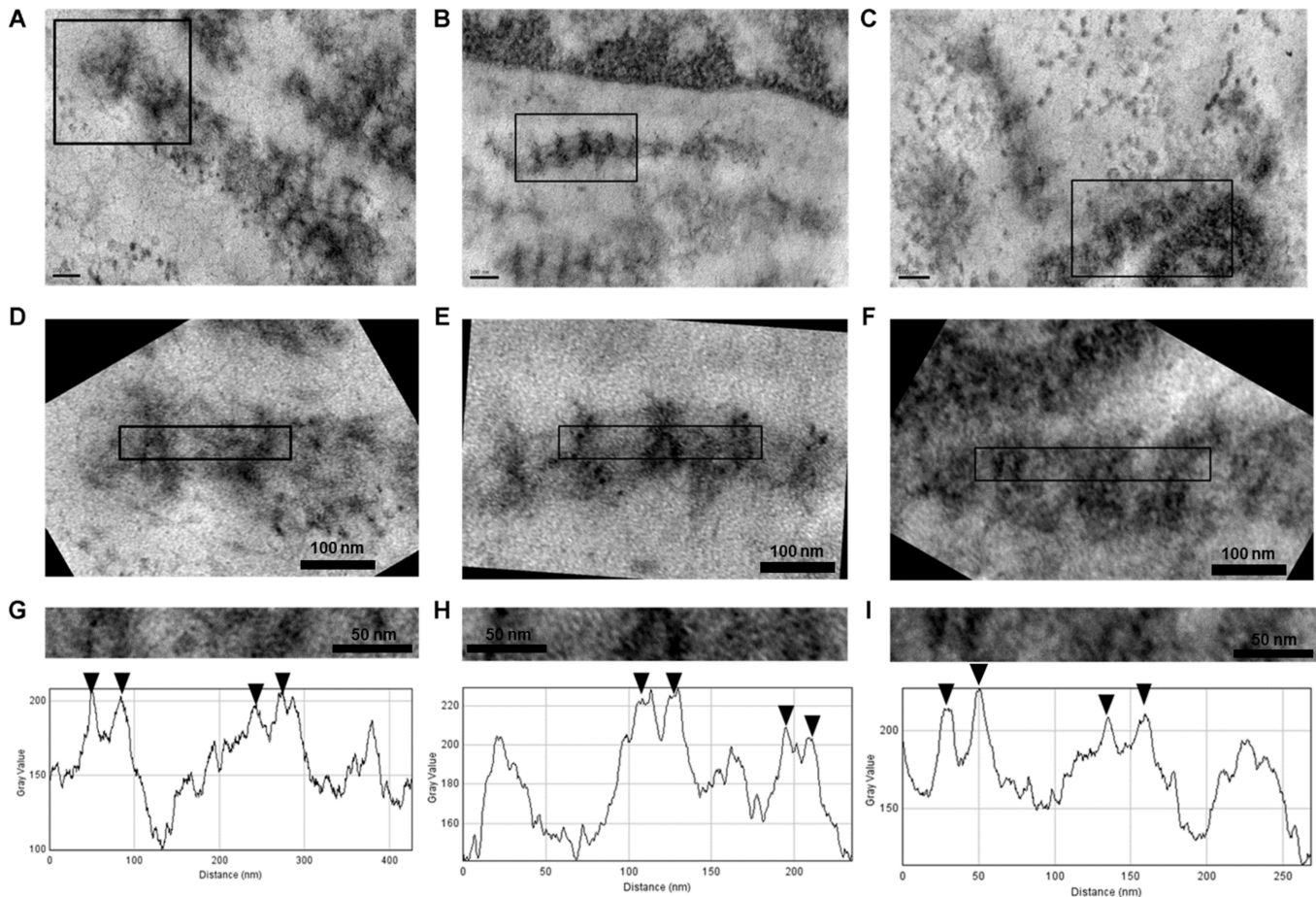


Figure 4. Representative collagen VI assemblies showing pairs of transverse double bands. **A**, **B**, and **C**: Representative collagen VI assemblies found in the human trabecular meshwork during this study (scale bars = 100 nm). The boxed regions in **A**, **B**, and **C** are magnified in **D**, **E**, and **F** (scale bars = 100 nm). **G**, **H**, and **I**: A magnified view and profile density plot of the boxed regions in **D**, **E**, and **F** (scale bars = 50 nm). The horizontal axis of the plots corresponds to distance along the long axis of the rectangular selections. The density profile was obtained by integrating the electron density in the rectangular selection along a vertical path. Arrows indicate peaks on the profile plots that correspond to the dark double transverse band of collagen VI assemblies.

by other investigators [46,47], who confirmed they were proteoglycans by specific enzyme digestion protocols. Proteoglycans were found to associate close to the N- and C- globular domains of type VI collagen as well as to the rod-like segments (Figure 6; see Appendix 4, Appendix 5, and Appendix 6). Moreover, proteoglycans seemed to vary in morphology and size, which is consistent with the fact that different types of proteoglycans can interact with collagen type VI aggregates [47-49]. There was also some evidence of interaction between separate assemblies leading to the formation of larger collagen VI complexes (e.g., Figure 6). In general, it can be seen that the alignment between distinct assemblies within a larger complex occurred by keeping the transverse bands in the axial register (Figure 5 and Figure 6; see Appendix 4, Appendix 5, and Appendix 6).

DISCUSSION

Type VI collagen can form morphologically distinct aggregates with molecular organization that appears to be related to tissue morphology and physiology [22-28]. Various human pathologies have been associated with collagen type VI [34,35], for example, Bethlem myopathy, an autosomal-dominant, inherited, muscular disorder [50]. There are also indications that type VI collagen assemblies are associated with eye disorders, such as age-related macular degeneration, the leading cause of blindness in the Western world, and Sorsby's fundus dystrophy [37,38]. Previous workers have demonstrated that collagen type VI is a key extracellular matrix component of the trabecular meshwork [51-53]. The current investigation is the first to study the architecture and association with proteoglycans of collagen type VI assemblies

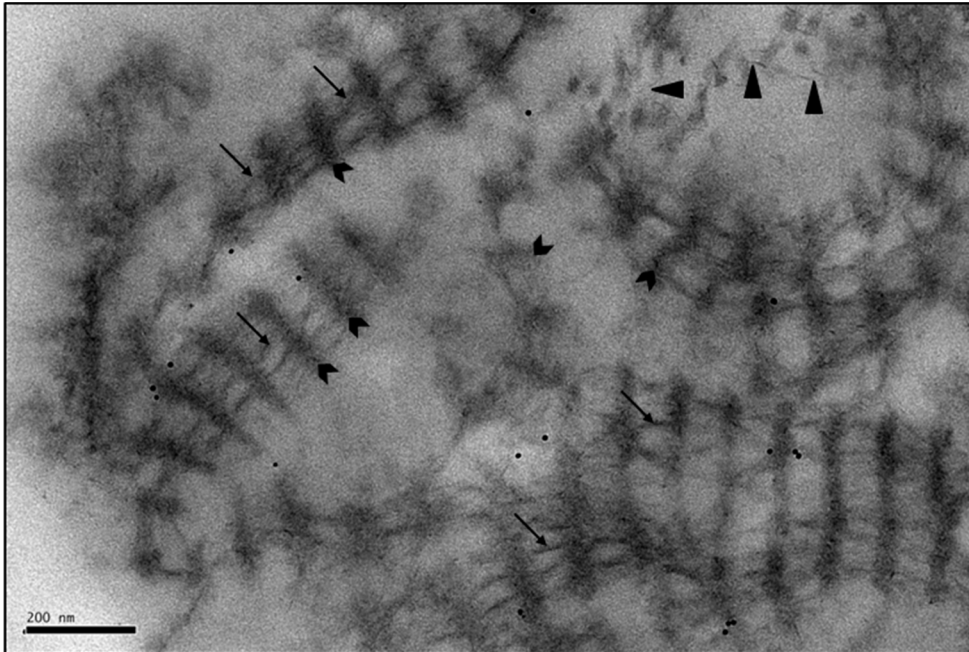


Figure 5. High-magnification longitudinal view of the type VI collagen aggregates in the trabecular sheets. Only single transverse bands are evident (chevrons), and their axial periodicity is approximately 109 nm. The rod-like segments of the collagen VI tetramers (arrows) cross the transverse bands at different angles. Proteoglycans are also seen in the matrix (arrowheads). Several 10-nm gold particles used for tomographic reconstruction appear as black dots in the electron micrograph. Scale bar = 200 nm.

in the human trabecular meshwork by three-dimensional electron tomography.

Our three-dimensional reconstructions showed that collagen type VI tetramers-identified as such from their morphology, periodicity, and the characteristic double-banded structure arising from the arrangement of the globular domains-were aggregated in a more disordered way

in the trabecular meshwork compared to other collagen type VI-rich tissues in which the collagen VI assemblies show an extended structural regularity [37,38,45]. This suggests that the molecular or physiologic environment of the trabecular meshwork matrix could interfere with the typical organization of collagen VI assemblies. Our proposed structural model for the collagen VI assemblies in the trabecular meshwork (Figure 7) was based on the interaction of collagen type

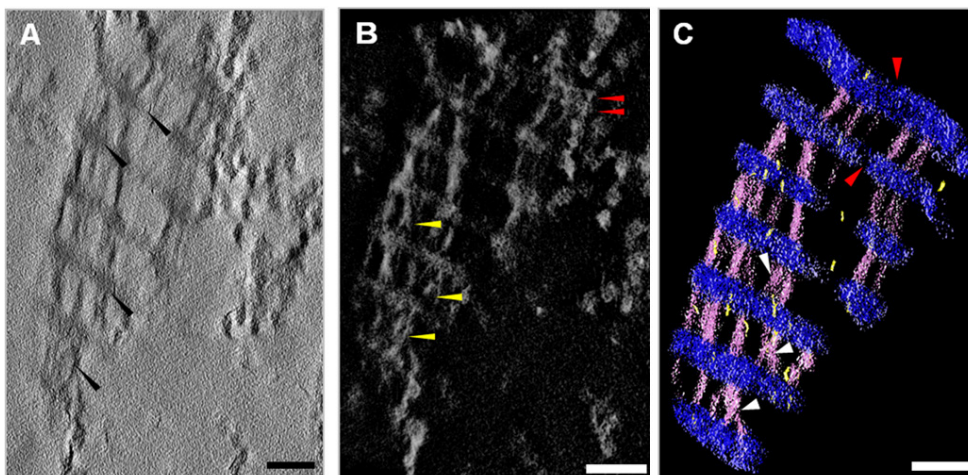


Figure 6. Tomographic reconstructions and segmentation of type VI collagen in the human trabecular meshwork. **A:** An 8.57-nm thick slice through a tomographic reconstruction of a collagen VI assembly. Arrowheads indicate proteoglycans interacting with collagen VI. **B:** Two-dimensional surface representation of a three-dimensional (3D) reconstruction. See Appendix 2 for a 360° view of the reconstruction. The 3D reconstruction has been contrast inverted, and therefore the

proteins are shown in white whereas the background is shown in black. The red arrowheads highlight two globular domains. The tetramer's rod-like segments (yellow arrowheads) run across the transverse bands and adopt an irregular organization. **C:** Manually segmented volume of the collagen VI assembly. See Appendix 5 for a 360° view. The transverse bands are shown in blue, the rod-like segments of the collagen VI tetramers in pink, and proteoglycans in yellow. Proteoglycans vary in size and interact with the collagen VI globular domains and the tetramer's rod-like segments. Scale bar = 100 nm.

VI tetramers through their globular domains. These interactions provide stability to the network of type VI collagen. Collagen VI tetramers are the building blocks in this model and they assemble together via noncovalent bonds between the N-terminal globular domains of one tetramer and the C-terminal globular domains of an adjacent tetramer. The electron dense mass of the globular domains would produce, in a different environment, two transverse bands at the position of the C- and N- terminal domains. The fact that single-banded assemblies were largely prevalent suggests that extra material accumulates in the space between the globular domains. It is possible that one or more of the proteins present in the trabecular meshwork interact with the N- and C-terminal globular domains or with the outer rod-like segments of the tetramers, explaining why double-banded aggregates are not always visible in the human trabecular meshwork. It is apparent from our data that there was no extended lateral regularity in the arrangement of the collagen type VI tetramers since not only was their separation variable but so were the relative angles that the inner and outer rod-like segments of the tetramers make with the transverse bands of the assemblies. This might be an effect of the ionic micro-environment of the trabecular matrix itself. In fact, trabecular meshwork cells have the potential to manipulate

the aqueous humor outflow by altering the extracellular ionic micro-environment of their matrix, modulating extracellular matrix composition [54], including, for example, the size and degree of extension of meshwork proteoglycans. Following the principle of ionic modulation of flow resistance by the trabecular meshwork cells, a simple supposition would be that changes in the physicochemical properties of the trabecular meshwork would also affect the interactions between the globular domains of the type VI collagen molecules. On this basis, interactions between the globular domains that hold together adjacent tetramers would be disturbed, and this would have an effect on the structural stability of collagen type VI aggregates.

A second possibility is that the structural irregularity of the collagen type VI assemblies in the human trabecular meshwork is the consequence of interactions between the N- and C-terminal domains, which are somehow modulated by other factors or molecules. We should also consider that trabecular meshwork cells sense changes in mechanical stress or intraocular pressure that might trigger remodeling of the matrix to adjust the outflow resistance and maintain intraocular pressure homeostasis. Several matrix proteins are often involved in reorganization of the extracellular matrix and changes in cell-matrix interactions, and some of

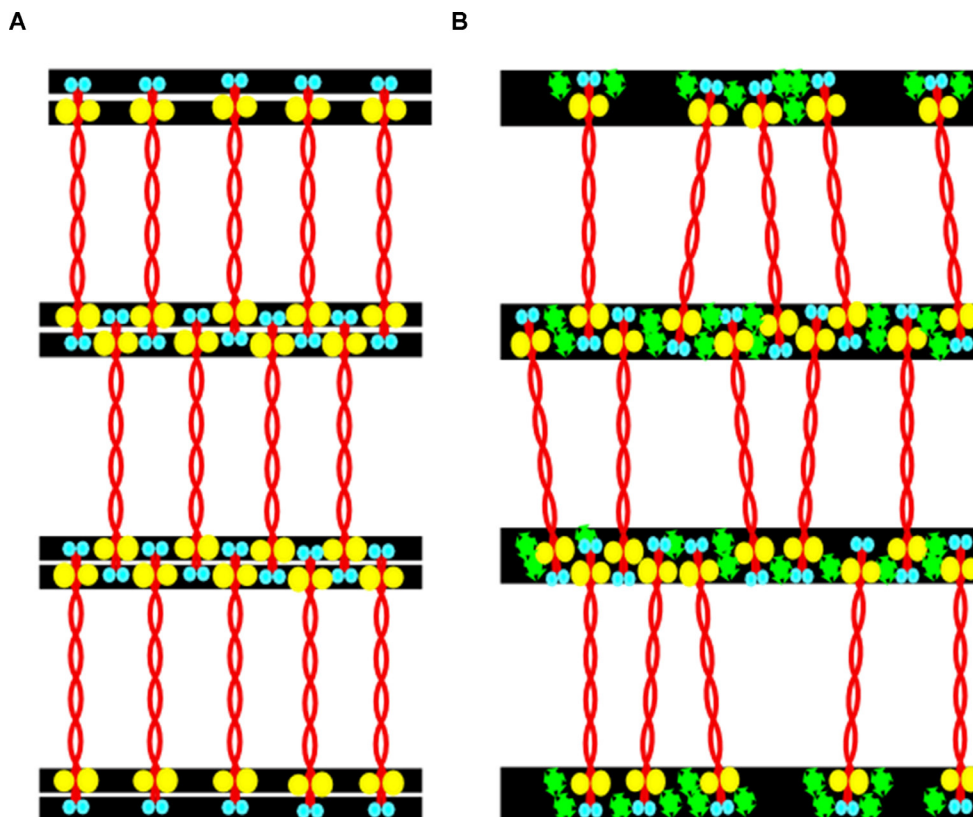


Figure 7. Schematic model of the collagen VI assembly found in human trabecular sheets. N and C termini are depicted in blue and yellow, respectively, and the collagenous triple helices in red. **A:** Model for the double-banded aggregates arising from the alignment of the N- and C-globular domains of the collagen VI tetramers. The black rectangles highlight the position of the transverse bands as seen in the electron micrographs. **B:** Model for the assemblies presenting a single transverse band. The single band arises from a double band with extra material (in green) filling the spaces between globular domains.

these proteins may interact with the collagen VI assemblies. Sulfated proteoglycans have been documented previously in the human trabecular meshwork where they interact with fibrillar collagen [55] and are likely to contribute to aqueous outflow resistance. Here, we demonstrated that these negatively charged macromolecules co-associate with collagen type VI assemblies. In a three-dimensional view, it is clear that while the binding site for a proportion of proteoglycans was located on rod-like segments of the collagen VI tetramers, there were also some proteoglycans associated with the transverse bands where the globular domains of collagen type VI are found. Our findings align with other studies that have shown that collagen type VI interacts with membrane-associated chondroitin sulfate proteoglycan [48], and also with biglycan and decorin [47,49], members of the small leucine-rich repeat proteoglycan family. The interaction of NG2 and collagen type VI is thought to be important in extracellular matrix organization as well as in cell-matrix interactions that determine cell morphology with respect to the matrix. The possibility of multiple proteoglycan binding sites is also in line with previous investigations, indicating that biglycan and decorin are localized near the N-terminal region of the triple helical domain [56] and the following globular domain of type VI collagen tetramers. Previous studies of human trabecular meshwork have indicated a decrease in the numbers of stained cuprolinic blue-proteoglycan complexes with age [47] but an increase in the amount of collagen type VI [57]. These age-related alterations in matrix composition might influence the molecular ultrastructure and interactions in the human trabecular meshwork. It is hoped that new insights into the structure of collagen type VI and associated matrix structures of the trabecular meshwork in the three-dimensional view will shed more light on the function of the tissue and its role in the outflow pathway. As was previously mentioned, the human trabecular meshwork provides flow resistance to aqueous humor leaving the anterior chamber of the eye and thus likely plays a role in the regulation of intraocular pressure [39]. If collagen type VI plays a role in the maintenance of the aqueous humor outflow pathway in the trabecular meshwork, one might hypothesize that alterations in its ultrastructure and interactions with other extracellular matrix components might impact upon pathological changes in the trabecular meshwork.

APPENDIX 1. 3D SURFACE-RENDERED RECONSTRUCTION OF TYPE VI COLLAGEN AGGREGATES IN THE HUMAN TRABECULAR MESHWORK.

To access the data, click or select the words “[Appendix 1.](#)” The image has been contrast inverted and therefore the proteins are shown in white whereas the background is shown in black.

APPENDIX 2. A SURFACE REPRESENTATION OF A 3D RECONSTRUCTION OF THE TILTED TYPE VI COLLAGEN AGGREGATES.

To access the data, click or select the words “[Appendix 2.](#)” A tilt series was acquired by tilting the specimen around a single tilt axis, in two degree increments over a limited tilt range (+60°, - 60°). See Appendix 3 to view the entire tilt series. The image stack has been contrast-inverted and therefore the proteins are shown in white whereas the background is shown in black. The red arrowheads highlight the double dark transverse bands, formed by N- and C- globular domains of type VI collagen. This feature of collagen VI is not clearly seen in two-dimensional projections. The collagenous triple-helices (yellow arrowheads) run nearly perpendicular to the dark bands.

APPENDIX 3. 3D SURFACE RECONSTRUCTION OF MULTIPLE TYPE VI COLLAGEN AGGREGATES IN THE HUMAN TRABECULAR MESHWORK.

To access the data, click or select the words “[Appendix 3.](#)” The image has been contrast-inverted and therefore the proteins are shown in white whereas the background is shown in black.

APPENDIX 4. TOMOGRAPHIC RECONSTRUCTION AND SEGMENTATION OF TYPE VI COLLAGEN MOLECULES IN THE HUMAN TRABECULAR MESHWORK.

To access the data, click or select the words “[Appendix 4.](#)” Appendix 6 to view the entire tilt series and the segmented reconstructed volume. (A) Still image from a single slice through a tomographic reconstruction. (B) Manually-segmented reconstructed volume of the collagen VI molecules and proteoglycans, depicted in (A). The dark transverse bands (N- and C- globular domains) are shown in blue, the collagenous triple-helices in pink, and proteoglycans in yellow. Proteoglycans vary in size and interact with the terminal globular domains and/or the triple helices (purple

arrowheads). White arrowheads point to interacting collagenous domains. Lateral associations of adjacent aggregates are indicated by the green arrowheads. A red arrowhead indicates a double band, characteristic of collagen VI. Scale bar=100 nm.

APPENDIX 5. MANUALLY-SEGMENTED RECONSTRUCTED VOLUME OF THE COLLAGEN VI MOLECULES AND PROTEOGLYCAN IN THE AGGREGATES.

To access the data, click or select the words “[Appendix 5.](#)” The globular domains are shown in blue, the collagenous triple-helices in pink and the proteoglycans in yellow. This reconstruction was generated by acquiring a tilt series at one degree increments over a tilt range in both directions (+60°, -60°).

APPENDIX 6. MANUALLY-SEGMENTED RECONSTRUCTED VOLUME OF THE AGGREGATES IN APPENDIX 3.

To access the data, click or select the words “[Appendix 6.](#)” The globular domains are shown in blue, the collagenous triple-helices in pink and the proteoglycans in yellow.

ACKNOWLEDGMENTS

This work was supported by a Cardiff University Professor Sir Martin Evans’ President’s Studentship to EK, and by collaborative research grants from the Japan Society for the Promotion of Sciences and the Japan Eye Bank.

REFERENCES

- Kielty CM, Hopkinson I, Grant ME. Connective tissue and its heritable disorders: Molecular, Genetic and Medical aspects, 2nd ed. Royce, P.M., Steinmann, B.(Eds.), NJ, USA, 2003. pp. 190–2
- Trüeb B, Schreier T, Bruckner P, Winterhalter KH. Type VI collagen represents a major fraction of connective tissue collagens. *Eur J Biochem* 1987; 166:699-03. [PMID: 3111851].
- Keene DR, Engvall E, Glanville RW. Ultrastructure of type VI collagen in human skin and cartilage suggest an anchoring function for this filamentous network. *J Cell Biol* 1988; 107:1995-06. [PMID: 3182942].
- Chung E, Rhodes K, Miller EJ. Isolation of three collagenous components of probable basement membrane origin from several tissues. *Biochem Biophys Res Commun* 1976; 71:1167-74. [PMID: 971306].
- Odermatt E, Risteli J, van Delden V, Timpl. Structural diversity and domain composition of a unique collagenous fragment (intima collagen) obtained from human placenta. *Biochem J* 1983; 211:295-02. [PMID: 6870834].
- Furthmayr H, Wiedemann H, Timpl R, Odermatt E, Engel J. Electron- microscopical approach to a structural model of intima collagen. *Biochem J* 1983; 211:303-11. [PMID: 6307276].
- von der Mark H, Aumailley M, Wick G, Fleischmajer R, Timpl R. Immunocytochemistry, genuine size and tissue localization of collagen VI. *Eur J Biochem* 1984; 142:493-02. [PMID: 6432530].
- Hessle H, Engvall E, Type VI. Collagen. Studies on its localization, structure, and biosynthetic form with monoclonal antibodies. *J Biol Chem* 1984; 259:3955-61. [PMID: 6368554].
- Engel J, Furthmayr H, Odermatt E, von der Mark H, Aumailley M, Fleischmajer R, Timpl R. Structure and macromolecular organization of type VI collagen. *Ann N Y Acad Sci* 1985; 460:25-37. [PMID: 3938630].
- Kuo HJ, Keene DR, Glanville RW. The macromolecular structure of type-VI collagen. Formation and stability of filaments. *Eur J Biochem* 1995; 232:364-72. [PMID: 7556183].
- Knupp C, Squire JM. A new twist in the collagen story- the type VI segmented supercoil. *EMBO J* 2001; 20:372-6. [PMID: 11157744].
- Knupp C, Pinali C, Munro PM, Gruber HE, Sherratt MJ, Baldock C, Squire JM. Structural correlation between collagen VI microfibrils and collagen VI banded aggregates. *J Struct Biol* 2006; 154:312-26. [PMID: 16713302].
- Meek KM, Fullwood NJ. Corneal and scleral collagens—a microscopist’s perspective. *Micron* 2001; 32:261-72. [PMID: 11006506].
- Jander R, Rauterberg J, Glanville RW. Further characterization of the three polypeptide chains of bovine and human short-chain collagen (intima collagen). *Eur J Biochem* 1983; 133:39-46. [PMID: 6852033].
- Chu ML, Conway D, Pan TC, Baldwin C, Mann K, Deutzmann R, Timpl R. Amino acid sequence of the triple-helical domain of human collagen type VI. *J Biol Chem* 1988; 263:18601-6. [PMID: 3198591].
- Fitzgerald J, Rich C, Zhou FH, Hansen U. Three novel collagen VI chains, alpha4(VI), alpha5(VI), and alpha6(VI). *J Biol Chem* 2008; 283:20170-80. [PMID: 18400749].
- Gara SK, Grumati P, Urciuolo A, Bonaldo P, Kobbe B, Koch M, Paulsson M, Wagener R. Three novel collagen VI chains with high homology to the alpha3 chain. *J Biol Chem* 2008; 283:10658-70. [PMID: 18276594].
- Bruns RR. Beaded filaments and long-spacing fibrils: relation to type VI collagen. *J Ultrastruct Res* 1984; 89:136-45. [PMID: 6100555].
- Ayad S. The extracellular matrix facts book. Academic Press, London, UK, 1994.
- Wu JJ, Eyre DR, Slayter HS. Type VI collagen of the intervertebral disc. *Biochemical and electron-microscopic*

- characterization of the native protein. *Biochem J* 1987; 248:373-81. [PMID: 3124811].
21. Knupp C, Squire JM. Molecular packing in network-forming collagens. *Adv Protein Chem* 2005; 70:375-03. [PMID: 15837521].
 22. Reale E, Groos S, Luciano L, Eckardt C, Eckardt U. In the mammalian eye type VI collagen tetramers form three morphologically different aggregates. *Matrix Biol* 2001; 20:37-51. [PMID: 11246002].
 23. Linsenmayer TF, Mentzer A, Irwin MH, Waldrep NK, Mayne R. Avian type VI collagen. Monoclonal antibody production and immunohistochemical identification as a major connective tissue component of cornea and skeletal muscle. *Exp Cell Res* 1986; 165:518-29. [PMID: 3522257].
 24. Hirano K, Kobayashi M, Kobayashi K, Hoshino T, Awaya S. Experimental formation of 100 nm periodic fibrils in the mouse corneal stroma and trabecular meshwork. *Invest Ophthalmol Vis Sci* 1989; 30:869-74. [PMID: 2722443].
 25. Shuttleworth CA, Berry L, Kielty CM. Microfibrillar components in dental pulp: presence of both type VI collagen and fibrillin-containing microfibrils. *Arch Oral Biol* 1992; 37:1079-84. [PMID: 1471956].
 26. Rittig M, Lütjen-Drecoll E, Rauterberg J, Jander R, Mollenhauer J. Type-VI collagen in the human iris and ciliary body. *Cell Tissue Res* 1990; 259:305-12. [PMID: 2337925].
 27. Garron LK, Feeney ML. Electron microscopic studies of the human eye. II. Study of the trabeculae by light and electron microscopy. *Arch Ophthalmol* 1959; 62:966-73. [PMID: 13855820].
 28. Leeson TS, Speakman JS. The fine extracellular material in the pectinate ligament (trabecular meshwork) of the human iris. *Acta Anat (Basel)* 1961; 46:363-79. [PMID: 14463630].
 29. Specks U, Mayer U, Nischt R, Spissinger T, Mann K, Timpl R, Engel J, Chu ML. Structure of recombinant N-terminal globule of type VI collagen alpha 3 chain and its binding to heparin and hyaluronan. *EMBO J* 1992; 11:4281-90. [PMID: 1425570].
 30. Burg MA, Tillet E, Timpl R, Stallcup WB. Binding of the NG2 proteoglycan to type VI collagen and other extracellular matrix molecules. *J Biol Chem* 1996; 271:26110-6. [PMID: 8824254].
 31. Sabatelli P, Bonaldo P, Lattanzi G, Braghetta P, Bergamin N, Capanni C, Mattioli E, Columbaro M, Ognibene A, Pepe G, Bertini E, Merlini L, Maraldi NM, Squarzone S. Collagen VI deficiency affects the organization of fibronectin in the extracellular matrix of cultured fibroblasts. *Matrix Biol* 2001; 20:475-86. [PMID: 11691587].
 32. Wiberg C, Klatt AR, Wagener R, Paulsson M, Bateman JF, Heinegård D, Mörgelin M. Complexes of matrilin-1 and biglycan or decorin connect collagen VI microfibrils to both collagen II and aggrecan. *J Biol Chem* 2003; 278:37698-04. [PMID: 12840020].
 33. Kuo HJ, Maslen CL, Keene DR, Glanville RW. Type VI collagen anchors endothelial basement membranes by interacting with type IV collagen. *J Biol Chem* 1997; 272:26522-9. [PMID: 9334230].
 34. Pepe G, Bertini E, Giusti B, Brunelli T, Comeglio P, Saitta B, Merlini L, Chu ML, Federici G, Abbate R. A novel de novo mutation in the triple helix of the COL6A3 gene in a two-generation Italian family affected by Bethlem myopathy. A diagnostic approach in the mutations' screening of type VI collagen. *Neuromuscul Disord* 1999; 9:264-71. [PMID: 10399756].
 35. Lampe AK, Dunn D, von Niederhausern AC, Hamil C, Aoyagi A, Laval SH, Marie SK, Chu ML, Swoboda K, Muntoni F, Bonnemann CG, Flanigan KM, Bushby KM, Weiss RB. Automated genomic sequence analysis of the three collagen VI genes: applications to Ullrich congenital muscular dystrophy and Bethlem myopathy. *J Med Genet* 2005; 42:108-20. [PMID: 15689448].
 36. Scacheri PC, Gillanders EM, Subramony SH, Vedanarayanan V, Crowe CA, Thakore N, Bingler M, Hoffman EP. Novel mutations in collagen VI genes: expansion of the Bethlem myopathy phenotype. *Neurology* 2002; 58:593-02. [PMID: 11865138].
 37. Knupp C, Amin SZ, Munro PM, Luthert PJ, Squire JM. Collagen VI assemblies in age-related macular degeneration. *J Struct Biol* 2002; 139:181-9. [PMID: 12457848].
 38. Knupp C, Chong NH, Munro PM, Luthert PJ, Squire JM. Analysis of the collagen VI assemblies associated with Sorby's Fundus Dystrophy. *J Struct Biol* 2002; 137:31-40. [PMID: 12064931].
 39. Bill A, Maepea O. Mechanisms and routes of aqueous humor drainage. In *Principles and Practices of Ophthalmology* Philadelphia. W B Saunders, DM Albert, FA Jakotiec, 1994. pp. 206-226.
 40. Kremer JR, Mastrorade DN, McIntosh JR. Computer visualization of three-dimensional image data using IMOD. *J Struct Biol* 1996; 116:71-6. [PMID: 8742726].
 41. Ress DB, Harlow ML, Marshall RM, McMahan UJ. Methods for generating high-resolution structural models from electron microscope tomography data. *Structure* 2004; 12:1763-74. [PMID: 15458626].
 42. Schmid B, Schindelin J, Cardona A, Longair M, Heisenberg M. A high-level 3D visualization API for Java and ImageJ. *BMC Bioinformatics* 2010; 11:274-[PMID: 20492697].
 43. Schneider CA, Rasband WS, Eliceiri KW. NIH Image to ImageJ: 25 years of image analysis. *Nat Methods* 2012; 9:671-5. [PMID: 22930834].
 44. Hirano K, Kobayashi M, Kobayashi K, Hoshino T, Awayo S. Experimental formation of 100 nm periodic fibrils in the mouse corneal stroma and trabecular meshwork. *Invest Ophthalmol Vis Sci* 1989; 30:869-74. [PMID: 2722443].
 45. Knupp C, Munro PMG, Luther PK, Ezra E, Squire JM. Structure of abnormal molecular assemblies (collagen VI) associated with human full thickness macular holes. *J Struct Biol* 2000; 129:38-47. [PMID: 10675295].

46. Tawara A, Varner HH, Hollyfield JG. Distribution and characterization of sulfated proteoglycans in the human trabecular meshwork. *Invest Ophthalmol Vis Sci* 1989; 10:2215-31. .
47. Gong H, Freddo TF, Johnson M. Age-related changes of sulfated proteoglycans in the normal human trabecular meshwork. *Exp Eye Res* 1992; 55:691-709. [PMID: 1478279].
48. Sallcup WB, Dahlin K, Healy P. Interaction of the NG2 chondroitin sulfate proteoglycan with type VI collagen. *J Cell Biol* 1990; 11:3177-88. .
49. Bidanset DJ, Guidry C, Rosenberg LC, Choi HU, Timpl R, Hook M. Binding of the proteoglycan decorin to collagen type VI. *J Biol Chem* 1992; 267:5250-6. [PMID: 1544908].
50. Acott TS, Kelley MJ. Extracellular matrix in the trabecular meshwork. *Exp Eye Res* 2008; 86:543-61. [PMID: 18313051].
51. Bethlem J, Wijngaarden GK. Benign myopathy, with autosomal dominant inheritance. A report on three pedigrees. *Brain* 1976; 99:91-100. [PMID: 963533].
52. Lütjen-Drecoll E, Rittig M, Rauterberg J, Jander R, Mollenhauer J. Immunomicroscopical study of type VI Collagen in the trabecular meshwork of normal and glaucomatous eyes. *Exp Eye Res* 1989; 48:139-47. [PMID: 2920781].
53. Marshall GE, Konstas AG, Lee WR. Immunogold ultrastructural localization of collagens in the aged human outflow system. *Ophthalmology* 1991; 98:692-700. [PMID: 2062503].
54. Ueda J, Wentz-Hunter K, Yue BY. Distribution of myocilin and extracellular matrix components in the juxtacanalicular tissue of human eyes. *Invest Ophthalmol Vis Sci* 2002; 43:1068-76. [PMID: 11923248].
55. Gard TL, Van Buskirk EM, Acott TS. Ionic modulation of flow resistance in an immobilized proteoglycan model of the trabecular meshwork. *J Glaucoma* 1993; 2:183-92. [PMID: 19920516].
56. Wiberg C, Hedbom E, Khairullina A, Lamandé SR, Oldberg A, Timpl R, Mörgelin M, Heinegård D. Biglycan and Decorin bind close to the N-terminal region of the collagen VI triple helix. *J Biol Chem* 2001; 276:18947-52. [PMID: 11259413].
57. Millard CB, Tripathi BJ, Tripathi RC. Age-related changes in protein profiles of the normal human trabecular meshwork. *Exp Eye Res* 1987; 45:623-31. [PMID: 3428388].

Articles are provided courtesy of Emory University and the Zhongshan Ophthalmic Center, Sun Yat-sen University, P.R. China. The print version of this article was created on 13 May 2014. This reflects all typographical corrections and errata to the article through that date. Details of any changes may be found in the online version of the article.